

identical conclusions follow from studies of other triarylmethyl systems,²ⁱ triarylboranes,^{2b} and triaryl amines.³⁴

Acknowledgment. We are indebted to Professors

(34) D. Hellwinkel, M. Melan, and C. R. Degel, *Tetrahedron*, **29**, 1895 (1973).

Paul v. R. Schleyer and W. Todd Wipke for access to strain programs developed in their respective research groups which aided in the formulation of our own computer program. We would also like to thank Princeton University for a generous allotment of computer time.

Stereochemistry of Dimesityl-9-anthrylmethane and Bis(2,6-xylyl)-1-(2-methylnaphthyl)methane. Evidence for the Two-Ring Flip Mechanism in Triarylmethanes¹

Paolo Finocchiaro,² Devens Gust, and Kurt Mislow*

Contribution from the Department of Chemistry, Princeton University, Princeton, New Jersey 08540. Received August 16, 1973

Abstract: The temperature-dependent ¹H-nmr spectra of the title compounds indicate that these molecules adopt a propeller conformation in the ground state, and that a variety of interconversions of stereoisomeric molecules on the nmr time scale occurs at elevated temperatures. These interconversions are all shown to proceed by the two-ring flip mechanism. The associated free energies of activation are reported. Comparison of the present results with the results of earlier studies on triarylmethanes, triarylboranes, and cognates brings to light that the two-ring flip mechanism is the favored stereoisomerization pathway for all of these systems.

The previous papers in this series³ discussed the stereochemistry of trimesitylmethane (**1**), which represents the simplest stereochemical class of triarylmethanes in that all three aryl groups are the same and possess local C₂ axes. Since the degeneracies inherent in this system do not permit the assignment of a stereoisomerization mechanism solely on the basis of nmr spectroscopic evidence, ancillary arguments were needed.

The present report deals with stereoisomerism and stereoisomerization in two triarylmethane systems of greater complexity, dimesityl-9-anthrylmethane (**2**) and bis(2,6-xylyl)-1-(2-methylnaphthyl)methane (**3**). The analysis of stereoisomerization for these two systems is somewhat more involved than that for **1**, but by the same token yields more mechanistic information, and allows assignment of stereoisomerization mechanisms on nmr spectroscopic evidence alone. In addition, this study allows a comparison between the stereochemistry of **2** and **3** and that of their boron analogs, whose properties have been reported earlier.⁴

Dimesityl-9-anthrylmethane (2). By analogy with **1** and related compounds,³ **2** and **3** are both presumed to adopt the propeller conformation in the ground state. The sense of twist of the propeller may be either right- or left-handed, and **2** therefore exists in two enantiomeric forms, similar to the case of **1**.³ However, one of the degeneracies present in **1** (a C₃ molecule) has been removed by replacing one mesityl group by a 9-anthryl

group. Thus **2** is asymmetric (even though all three rings possess local C₂ axes and two of the rings are the same), and all four of the *o*-methyl groups of each enantiomer are diastereotopic, as are the two *p*-methyl groups. In the absence of accidental isochrony, the ¹H-nmr spectrum of **2** in an achiral medium should therefore feature four signals for the *o*-methyl groups and two for the *p*-methyl groups.

At 23° the 60-MHz ¹H-nmr spectrum of a CHBr₃ solution of **2** displays five methyl resonances in a ratio of intensities of ca. 2:1:1:1:1 (Figure 1). The four up-field resonances are due to the four diastereotopic *o*-methyl groups, which are shielded by the aromatic rings. The more intense downfield resonance is due to the two diastereotopic *p*-methyl groups, which are accidentally isochronous. The low-temperature spectrum is thus in accord with the postulated propeller conformation.

The possible stereoisomerization pathways for **2** may be divided into five classes: inversion along the C-H bond, and four classes of flip mechanisms.^{3,5} As in the case of **1**, each enantiomer of **2** has available one inversion, one zero-ring flip, and one three-ring flip pathway. However, in contrast to **1**, since the molecule no longer has C₃ symmetry the system is now capable of undergoing three discrete two-ring flips and three discrete one-ring flips.

These pathways are shown graphically in Figure 2. The two vertices represent the enantiomers of **2**, and the edges represent stereoisomerizations. The edges are

(1) This work was supported by the National Science Foundation (GP-30257).

(2) NATO Fellow, 1972-1973, on leave of absence from the University of Catania, Catania, Italy.

(3) (a) P. Finocchiaro, D. Gust, and K. Mislow, *J. Amer. Chem. Soc.*, **96**, 2165 (1974); (b) J. D. Andose and K. Mislow, *ibid.*, **96**, 2168 (1974).

(4) J. F. Blount, P. Finocchiaro, D. Gust, and K. Mislow, *J. Amer. Chem. Soc.*, **95**, 7019 (1973).

(5) (a) D. Gust and K. Mislow, *J. Amer. Chem. Soc.*, **95**, 1535 (1973).

(b) The flip rearrangements result both in permutations of ligand positions and in a change of helicity of the molecular propeller. Another set of rearrangements which do not involve a net change of helicity is conceivable. All the available evidence³ suggests that the flip pathways are of lowest energy, and consequently we have limited our discussion to that set.

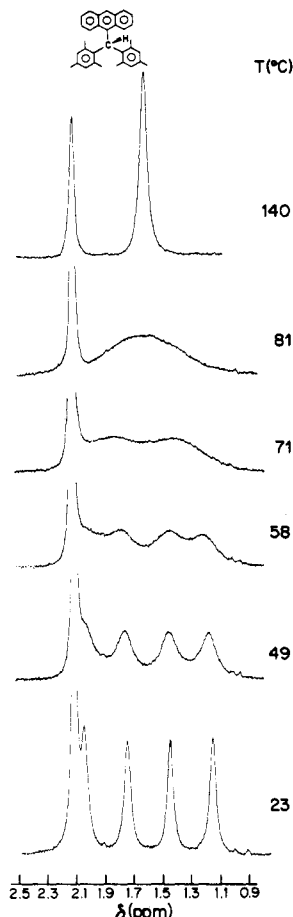


Figure 1. Temperature-dependent 60-MHz ^1H -nmr spectrum (methyl region) of **2**. The downfield peak (truncated in the temperature range 23–81 °C) corresponds to the *p*-methyl group resonances.

labeled with numerals identifying the rings which flip during the specified interconversion; for example, a two-ring flip of rings 1 and 2 is called a [1,2]-flip.⁶ Figure 2 illustrates the fact that although any one of the eight flip pathways results in enantiomerization, inversion does not, since this mechanism does not change the sense of twist (helicity) of the molecular propeller.⁵ The [1,2]- and [1,3]-flips are enantiomeric, as may be seen by an examination of the idealized transition states involved, and therefore they may be considered together in terms of the results, as indicated by the dashed box. A similar situation obtains in the case of the [2]- and [3]-flips.

Figure 2 also indicates the effect of stereoisomerizations by each pathway upon the methyl groups of **2**. Each of the methyl group environments is designated by a lower case letter in the structural formulas shown. Each edge of the graph is labeled with the environments of the methyl groups which are exchanged by the associated stereoisomerization. For all pathways except the enantiomeric one- and two-ring flips, these exchanges are readily determined by an examination of the idealized transition state in question. The result for the enantiomeric [1,2]- and [1,3]-flips (which necessarily occur at the same rate in an achiral medium) is

(6) Note that the reverse pathway would be a $[\bar{1},\bar{3}]$ -flip. The naming scheme employed in the text is based on the enantiomer shown on the left in Figure 2.

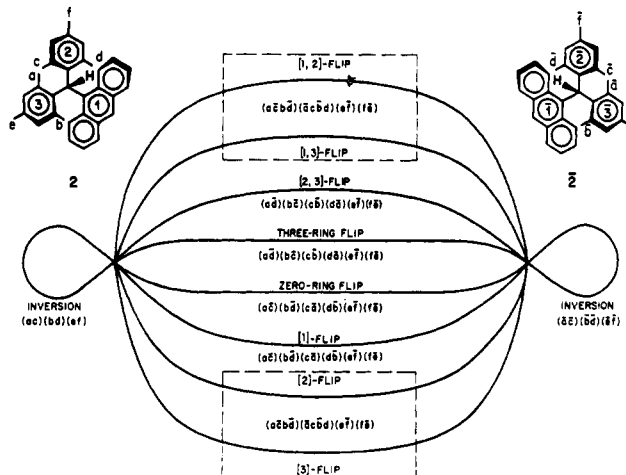


Figure 2. Graph depicting the possible stereoisomerizations of **2**. The environments of the methyl groups are labeled with lower case letters, and the numerals identify the aryl rings which flip during stereoisomerizations. A barred letter or numeral denotes an enantiomeric environment. The dashed boxes identify the two sets of enantiomeric flip mechanisms. Exchanged (permuted) environments are parenthesized.

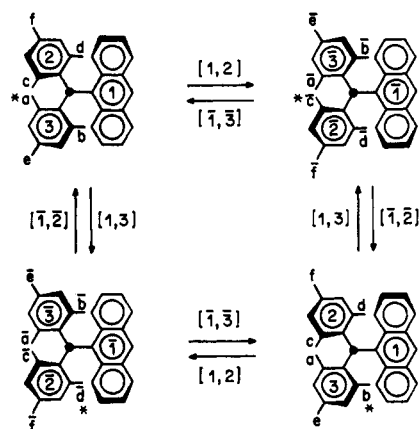


Figure 3. The effect of enantiomeric [1,2]- and [1,3]-flips on the interchange of environments (letters) of a given methyl group (asterisk) in **2**. The ring environments are numbered, and the numerals along the arrows identify the rings which flip during the specified interconversion. In the text, the flip pathways (undirected) are identified only by the unbarred designations.

most easily appreciated by use of Figure 3, in which one of the *o*-methyl groups has been labeled with an asterisk. During a succession of [1,2]- and [1,3]-flips this methyl group comes to reside in all four diastereomeric environments. A similar cycle can be constructed for the [2]- and [3]-flips.

These results provide a basis for the interpretation of stereoisomerizations of **2** which are revealed by its temperature-dependent nmr spectrum. As the nmr sample of **2** is warmed, the four *o*-methyl signals broaden and collapse to a singlet which becomes sharp at *ca.* 140 °C (Figure 1). The *p*-methyl signal remains essentially unchanged. This coalescence indicates stereoisomerization which is becoming rapid on the nmr time scale.

The mechanism of the observed stereoisomerization is necessarily one which results in simultaneous averaging of the environments of *all four* diastereotopic *o*-methyl groups. Figure 2 indicates that in the ab-

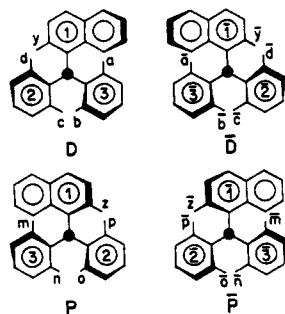


Figure 4. The four stereoisomers of **3** in the propeller conformation. The labeling scheme is similar to that used in Figures 2 and 3.

sence of fortuitously equivalent rates for two processes, only the enantiomeric [1,2]- and [1,3]-flips or the enantiomeric [2]- and [3]-flips account for this result, since all other mechanisms lead to coalescence of the four *o*-methyl signals to *two* signals, rather than to one. Thus, nmr evidence alone rules out all flip mechanisms other than the ones above.

If the results of the enantiomeric one-ring flips and two-ring flips are compared, an obvious difference is detected. In the propeller conformation, the protons in the 1 and 8 positions of the 9-anthryl group are diastereotopic; one is distal to the methine hydrogen and the other proximal. The enantiomeric [1,2]- and [1,3]-flips do not exchange these protons, but the [2]- and [3]-flips do, and thus, if the nmr resonances of these protons could be monitored, the correct mechanism would be deducible. Unfortunately, the complex spin pattern in the aromatic region has precluded a reliable determination for **2**. However, a previous study of a closely related compound provides the necessary information.

Dimesityl-1-(2,4,6-trimethoxyphenyl)methane (**4**) had been prepared and its temperature-dependent nmr spectrum studied by Martin and coworkers.⁷ These investigators had found that in the low-temperature limit the ¹H-nmr spectrum of **4** featured resonances for four *o*-methyl groups (two of which were accidentally isochronous) and two *o*-methoxy groups. Upon warming to *ca.* -20° the *o*-methyl group signals coalesced to a singlet, but the methoxy resonances remained distinct. Since **4** and **2** are both triarylmethanes in which two aryl groups are the same, and in which all three groups have local C₂ axes, they are stereochemically correspondent, and the analysis of stereoisomerism is therefore the same for both.⁸ This is illustrated, for example, by the fact that the graph in Figure 2 is isomorphic with the graph from our previous analysis^{5a} of **4**. However, the spectroscopically complex nmr resonances for the 1 and 8 protons of the anthryl group of **2** have been replaced by singlets for the *o*-methoxy groups of **4**. As we have previously pointed out,^{5a} since the *o*-methoxy signals of **4** do not coalesce with the same activation energy as the *o*-methyl resonances, the enantiomeric two-ring flips are the only flip pathways which are consistent with the experimental results. If we now assume that a similar situation obtains for **2**, we may rule out the [2]- and

[3]-flips for this compound as an explanation for the observed coalescence.

Granted that the two-ring flip is the lowest energy pathway for **2**, the energetics of the observed stereoisomerization may be estimated. The line shapes expected for the exchange of methyl groups of **2** by the [1,2]- and [1,3]-flips at various rates were calculated⁹ and fitted to the experimental spectra at eight temperatures. From these data, by use of the Eyring equation, a free energy of activation of $\Delta G^{\ddagger}_{77} = 17.2$ kcal/mol was calculated for the enantiomerization of **2** by the two-ring flip.

A comparison of the analyses of the conformational dynamics of **1**^{3a} and **2** clearly demonstrates that removal of just *one* degeneracy from the trimesityl-methane system (by replacement of a mesityl group with an anthryl group) has led to appreciably more mechanistic information. Whereas all stereoisomerization mechanisms other than the three-ring flip were in principle capable of serving as conceivable explanations of the observed site exchanges for **1**, only two pathways were found to be consistent with the temperature-dependent spectra of **2**. If it had been possible to analyze the anthryl group resonances, the remaining ambiguity could have been removed without the necessity of resorting to analogy with **4**. In addition, whereas it was not possible to rule out enantiomerization by the three-ring flip mechanism for **1**,^{3a} the results for **2** unequivocally eliminate this mechanism from consideration as the enantiomerization pathway of lowest energy (threshold mechanism^{8a}).

Would further removal of degeneracies yield yet more mechanistic information? To answer this question, we turned to the study of a more complex system in which *two* of the degeneracies present in **1** have been removed. This study is discussed in the following section.

Bis(2,6-xylyl)-1-(2-methylnaphthyl)methane (**3**).

This compound is a representative of the class of triarylmethanes having two identical aryl groups with local C₂ axes and a third aryl group which lacks such an axis. Since the 2-methyl-1-naphthyl group has no local C₂ axis, two diastereomers may exist,^{5a} one in which the naphthyl methyl group is proximal to the methine hydrogen (P) and a second in which the methyl group is distal (D). A given molecule of **3** may have a right- or left-handed sense of propeller helicity, and therefore each diastereomer exists as a *dl* pair. The four stereoisomers of **3** (P, \bar{P} , D, \bar{D} , where a bar designates an enantiomeric conformation) are depicted in Figure 4.

Each stereoisomer of **3** is asymmetric, and all four *o*-methyl groups on the xylyl rings of each diastereomer are therefore diastereotopic. This condition is reflected in the ambient temperature 100-MHz ¹H-nmr spectrum of a 1,2,4-trichlorobenzene solution of **3** (Figure 5): ten methyl signals are in evidence, as required by the above analysis.

(9) The computer program used was adapted from one developed by M. Saunders (see M. Saunders in "Magnetic Resonance in Biological Systems," A. Ehrenberg, B. C. Malmström, and T. Vängård, Ed., Pergamon Press, New York, N. Y., 1967, p 85). We are grateful to Professor Saunders for providing us with a copy of the program, and to Dr. Joseph D. Andose for the modifications. Calculations were performed using the facilities of the Princeton Computer Graphics Laboratory (E & S LDS 1/DEC PDP-10), supported in part by a grant from the National Institutes of Health.

(7) M. J. Sabacky, S. M. Johnson, J. C. Martin, and I. C. Paul, *J. Amer. Chem. Soc.*, **91**, 7542 (1969).

(8) K. Mislow, D. Gust, P. Finocchiaro, and R. J. Boettcher, *Fortschr. Chem. Forsch.*, **47**, 1 (1974).

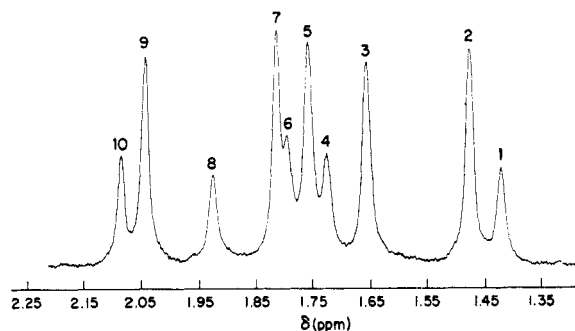


Figure 5. Ambient temperature (31 °C) 100-MHz ^1H -nmr spectrum (methyl region) of **3**. Numerals identify individual resonances; see text.

The five signals of higher intensity (numbered 2, 3, 5, 7, and 9) correspond to the methyl groups of the major diastereomer (**3a** and its enantiomer **3a**), whereas the resonances of lesser intensity (numbered 1, 4, 6, 8, and 10) are due to the minor diastereomer (**3b** and **3b**). One of these diastereomers necessarily corresponds to $\text{P}\bar{\text{P}}$ and the other to $\text{D}\bar{\text{D}}$, but we have no reliable basis on which to make an assignment. Coalescence data, which will be discussed later, have allowed us to identify resonances 7 and 10 as being due to the naphthyl methyl groups of their respective diastereomers. The other eight signals therefore correspond to xylyl methyl resonances. At 31 °C the population ratio of **3a**/**a** to **3b**/**b** is 2.05:1, as determined from relative peak intensities. This corresponds to a free energy for the equilibrium $\text{3a}/\bar{\text{a}} \rightleftharpoons \text{3b}/\bar{\text{b}}$ of $\Delta G^\circ_{31} = 0.43$ kcal/mol.

The possible stereoisomerization pathways of the isomers of **3** by the flip mechanisms will now be enumerated. These mechanisms belong to the same five classes as those described for **2**. As in **2**, each isomer has available eight flip pathways as well as one inversion. Figure 6 is a graph representing stereoisomerizations of the isomers of **3** by the flip mechanisms. The numbering and nomenclature refer to the structures in Figure 4. Since inversion is considered to be a high-energy pathway for triarylmethanes,^{3a} and was not observed for **2** and **4**, these pathways ($\text{P} \rightleftharpoons \text{D}$, $\bar{\text{P}} \rightleftharpoons \bar{\text{D}}$) have been omitted from the graph. The information in Figure 6 may be summed up by the statement that all pathways involving the flipping of the methylnaphthyl group (*i.e.*, flips including the numeral 1) lead to enantiomerization. All other pathways result in diastereomerization, since this necessarily involves the transfer of a naphthyl methyl group from a proximal to a distal position, or *vice versa*. Note that the zero-, [2]-, [3]- and [2,3]-flips which interconvert P and $\bar{\text{D}}$ are enantiomeric to the corresponding flips which interconvert $\bar{\text{P}}$ and D , and that in an achiral medium the rates of enantiomeric flips are the same. However, flips which enantiomerize P and $\bar{\text{P}}$ are diastereomeric to those which enantiomerize D and $\bar{\text{D}}$, and the two sets of flips are therefore expected to differ in energy. As was the case in **2**, [1,2]- and [1,3]-flips of $\text{P}\bar{\text{P}}$, as well as those of $\text{D}\bar{\text{D}}$ (dashed boxes in Figure 6), are enantiomeric, as may be seen by visualizing the idealized transition-state geometry for each interconversion. In contrast to **2**, however, the [2]- and [3]-flips of **3** are not enantiomeric, since the anthryl group (local C_2 axis) in

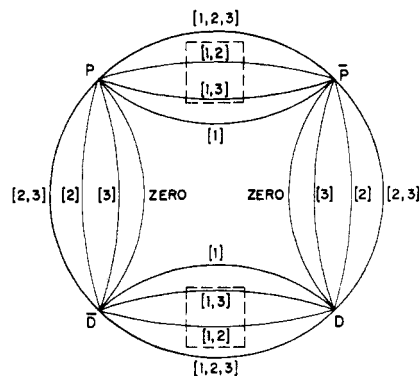


Figure 6. Graph depicting stereoisomerizations of **3** by the flip mechanisms. The dashed boxes identify the two sets of enantiomeric two-ring flip mechanisms. Refer to Figure 4 for significance of numerals and letters.

2 has been replaced by a 2-methyl-1-naphthyl group (no local C_2 axis) in **3**.

Table I lists the environments of the methyl groups of

Table I. Effect of Stereoisomerizations on the Environments of the Methyl Groups of **3**^a

Flip pathway	Resulting exchanges				
Diastereomerization					
$\text{D} \rightleftharpoons \bar{\text{P}}$ and $\bar{\text{D}} \rightleftharpoons \text{P}$					
Zero-ring flip	(a $\bar{\text{m}}$)	(b $\bar{\text{n}}$)	(c $\bar{\text{o}}$)	(d $\bar{\text{p}}$)	(y $\bar{\text{z}}$)
	($\bar{\text{a}}$ m)	($\bar{\text{b}}$ n)	($\bar{\text{c}}$ o)	($\bar{\text{d}}$ p)	($\bar{\text{y}}$ z)
[2]-flip	(a $\bar{\text{m}}$)	(b $\bar{\text{n}}$)	(c $\bar{\text{p}}$)	(d $\bar{\text{o}}$)	(y $\bar{\text{z}}$)
	($\bar{\text{a}}$ m)	($\bar{\text{b}}$ n)	($\bar{\text{c}}$ p)	($\bar{\text{d}}$ o)	($\bar{\text{y}}$ z)
[3]-flip	(a $\bar{\text{n}}$)	(b $\bar{\text{m}}$)	(c $\bar{\text{o}}$)	(d $\bar{\text{p}}$)	(y $\bar{\text{z}}$)
	($\bar{\text{a}}$ n)	($\bar{\text{b}}$ m)	($\bar{\text{c}}$ o)	($\bar{\text{d}}$ p)	($\bar{\text{y}}$ z)
[2,3]-flip	(a $\bar{\text{n}}$)	(b $\bar{\text{m}}$)	(c $\bar{\text{p}}$)	(d $\bar{\text{o}}$)	(y $\bar{\text{z}}$)
	($\bar{\text{a}}$ n)	($\bar{\text{b}}$ m)	($\bar{\text{c}}$ p)	($\bar{\text{d}}$ o)	($\bar{\text{y}}$ z)
Enantiomerizations					
$\text{D} \rightleftharpoons \bar{\text{D}}$					
[1]-flip	(a $\bar{\text{d}}$)	(b $\bar{\text{c}}$)	(c $\bar{\text{b}}$)	(d $\bar{\text{a}}$)	(y $\bar{\text{y}}$)
[1,2]- and [1,3]-flips	(a $\bar{\text{d}}$ b $\bar{\text{c}}$)	($\bar{\text{a}}$ d $\bar{\text{b}}$ c)		(y $\bar{\text{y}}$)	
[1,2,3]-flip	(a $\bar{\text{c}}$)	(b $\bar{\text{d}}$)	(c $\bar{\text{a}}$)	(d $\bar{\text{b}}$)	(y $\bar{\text{y}}$)
$\text{P} \rightleftharpoons \bar{\text{P}}$					
[1]-flip	(m $\bar{\text{p}}$)	(n $\bar{\text{o}}$)	(o $\bar{\text{n}}$)	(p $\bar{\text{m}}$)	(z $\bar{\text{z}}$)
[1,2]- and [1,3]-flips	(m $\bar{\text{p}}$ n $\bar{\text{o}}$)	($\bar{\text{m}}$ p $\bar{\text{n}}$ o)		(z $\bar{\text{z}}$)	
[1,2,3]-flip	(m $\bar{\text{o}}$)	(n $\bar{\text{p}}$)	(o $\bar{\text{m}}$)	(p $\bar{\text{n}}$)	(z $\bar{\text{z}}$)

^a See Figure 4 for explanation of numerals and letters.

the isomers of **3** which are exchanged by each flip pathway. These exchanges may be determined by examination of the idealized transition-state geometries, except in the case of the two sets of enantiomeric two-ring flips. The results in these two cases may be visualized most easily by use of cycles similar to that in Figure 3.

Figure 6 in conjunction with Table I may be used to interpret possible stereoisomerizations of **3** as revealed by the temperature-dependent nmr spectrum. As shown in Figure 7, warming of the nmr sample of **3** to *ca.* 72 °C results in exchange broadening of resonances 1, 4, 6, and 8. The two naphthyl methyl signals (7 and 10) are still sharp at this temperature. As was noted above, and as is also indicated in Table I, these two methyl groups are exchanged only during diastereomerization, and this process is therefore still slow on the nmr scale at 72 °C. Similarly, resonances 2, 3, 5, and 9

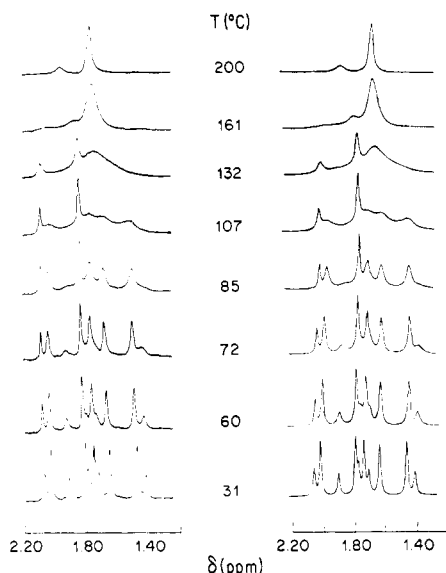


Figure 7. Temperature-dependent 100-MHz ^1H -NMR spectrum (methyl region) of **3** (left), and corresponding calculated spectra (right).

are still sharp, and therefore enantiomerization of **3a** and **3a** is slow. The observed broadening thus can only be due to enantiomerization of **3b** and **3b**. Of the three possible mechanisms for enantiomerization, the [1]-flip and the [1,2,3]-flip would each result in coalescence of four xylyl methyl signals to two signals, whereas the [1,2]- and [1,3]-flips would cause the simultaneous coalescence of all four resonances to a singlet. As the sample is warmed to *ca.* 90°, resonances 1, 4, 6, and 8 coalesce to a broad singlet. This coalescence must therefore result from interconversion of **3b** and **3b** by the enantiomeric [1,2]- and [1,3]-flips.

Similar behavior is observed for the major diastereomer. At about 85°, the four xylyl methyl resonances (2, 3, 5, and 9) begin to broaden, and further warming results in their coalescence to a broad singlet at *ca.* 132°. By reasoning similar to the above, it can be seen that the observed coalescence is due to enantiomerization of **3a** and **3a** by enantiomeric [1,2]- and [1,3]-flips. The enantiomeric two-ring flips are therefore the threshold mechanisms for enantiomerization of the isomers of **3**.

Figure 7 shows that at *ca.* 132° the naphthyl methyl group signals 7 and 10 begin to broaden, and have coalesced to a singlet which is beginning to sharpen at 200°. This coalescence is accompanied by the coalescence of all xylyl methyl group signals to a singlet. Such behavior is consistent only with diastereomerization (Table I). Any one of the four diastereomerization pathways is compatible with the experimental results when the rapid enantiomerizations discussed above are taken into account. Since the two threshold pathways are two-ring flips, it seems reasonable to postulate that the [2,3]-flip is responsible for the observed diastereoisomerization. This conclusion is supported by ancillary evidence which is brought out in the next section. It follows that *all three exchange processes are interpretable in terms of one class of mechanisms*.

The energetics of the observed processes may be

evaluated given the above mechanistic information. Reasonable fits were obtained using computer simulated spectra (Figure 7),⁹ yielding free energies of activation within satisfactory error limits. Free energy values of $\Delta G^\ddagger_{90} = 18.6$ kcal/mol and $\Delta G^\ddagger_{127} = 20.1$ kcal/mol were thus calculated for the enantiomerization of **3b/b** and **3a/a**, respectively. For the diastereomerization the calculations yielded $\Delta G^\ddagger_{161} = 22.3$ kcal/mol for the reaction **3b/b** \rightarrow **3a/a**, and $\Delta G^\ddagger_{161} = 22.9$ kcal/mol for the reverse reaction (**3a/a** \rightarrow **3b/b**).

Some Comparisons of Stereoisomerization Mechanisms among Diverse Propeller-Like Systems

The experimental results for **2** and **3**, when compared and contrasted with the results of other studies, bring to light some general aspects of stereoisomerization mechanisms in propeller molecules.

Effect of Steric Congestion on Threshold Barriers. The threshold barriers^{3a} for two-ring flips of **1**, **2**, **3**, and **4** span a wide range (*ca.* 13–22 kcal/mol) of activation energies (Table II). Since **2**, **3**, and **4** may be formally

Table II. Stereoisomerization Barriers for Selected Compounds^a

Compound	ΔG^\ddagger , kcal/ mol	Temp, °C	Ref
Trimesitylmethane (1)	21.9	167	3a
Dimesityl-9-anthrylmethane (2)	17.2	77	Present work
Bis(2,6-xylyl)-1-(2-methylnaphthyl)methane (3)	18.6 ^b	90	Present work
	20.1 ^c	127	
	22.3 ^d	161	
	22.9 ^e	161	
Dimesityl-1-(2,4,6-trimethoxyphenyl)methane (4)	~ 13 ^f	-20	7
	22.0 ^g	145	
Dimesityl-9-anthrylborane (9)	13.9	15	4
Dimesityl-1-(2-methylnaphthyl)borane (10)	15.4	20	4

^a All stereoisomerizations are interpreted in terms of two-ring flip mechanisms; where more than one barrier is listed, the lowest in energy refers to the threshold mechanism.^{3a} ^b Enantiomerization of **3b/b**. ^c Enantiomerization of **3a/a**. ^d Diastereomerization: **3b/b** \rightarrow **3a/a**. ^e Diastereomerization: **3a/a** \rightarrow **3b/b**. ^f Coalescence of mesityl *o*-methyl signals estimated from published data.⁷ ^g Coalescence of *o*-methoxy signals.

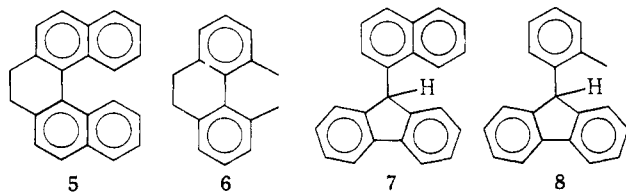
derived from trimesitylmethane by replacement of one mesityl group by another ligand to the central carbon atom (and noting that in the case of **3**, the remaining two mesityl groups are replaced with sterically similar 2,6-xylyl groups), these data permit the relative ordering of ligands in terms of their barrier-lowering attributes. To the extent that these attributes reflect steric hindrance in the two-ring flip, the ordering of relative "steric size" is therefore mesityl > 2-methyl-1-naphthyl > 9-anthryl > 2,4,6-trimethoxyphenyl. It is interesting to note in this connection that the barrier to racemization of **5** is $E_a = 30.8$ kcal/mol,¹⁰ whereas that for **6** is only *ca.* 23–25 kcal/mol.¹¹ Similarly, the barrier for diastereomerization of **7** is *ca.* 18–19 kcal/mol,¹²

(10) D. M. Hall and M. M. Harris, *J. Chem. Soc.*, 490 (1960).

(11) (a) K. Mislow and H. B. Hopps, *J. Amer. Chem. Soc.*, **84**, 3018 (1962); (b) O. Yamamoto and H. Nakanishi, *Tetrahedron*, **29**, 781 (1973).

(12) T. H. Siddall III and W. E. Stewart, *J. Org. Chem.*, **34**, 233 (1969).

whereas the barrier for **8** is *ca.* 16.3 kcal/mol.¹² In both of these cases, replacement of an *o*-methyl group by a benzo group results in an *increase* in activation energy, whereas in the case of the threshold mechanisms for **1**, **3** (either diastereomer), and **2**, successive replacements of a methyl group by a benzo group produce successive *decreases* in activation energy (Table II); a similar trend has been observed⁴ in the corresponding boranes (**9** and **10**, Table II). This divergent behavior, however, is hardly surprising, since ground and transition states for the enantiomerization of **1**, **2**, **3**, **9**, and **10**



are considerably different from those for stereomutation of **5**, **6**, **7**, and **8**. In the former, the transition states are two-ring flips, whereas in the latter, the transition states resemble more closely the zero-ring flip. The effective steric bulk of a group necessarily depends on the particular interaction in question, which in turn depends on the corresponding interconversion mechanism. The divergence in behavior is thus readily accounted for.

High-Energy Flip Mechanisms. Thus far we have been concerned only with threshold barriers. We will now direct our attention to additional stereoisomerization barriers of higher energy which were observed in compounds **3** and **4** (Table II). These barriers, and the barrier for **1**, are all nearly equal ($\Delta G^\ddagger = \text{ca. } 22 \text{ kcal/mol}$). This result helps to resolve a residual ambiguity in the interpretation of the temperature-dependent nmr behavior⁷ of **4**. As was earlier pointed out,^{5a} the nmr evidence alone does not rule out any one of three alternatives to the two-ring flip mechanism for the higher energy coalescence of **4**, *viz.*, inversion, the zero-ring flip, and the enantiomeric one-ring flips. Although the zero-ring flip and inversion were dismissed on energetic grounds,^{5a} it was not possible at that time to decide between the one- and two-ring flip mechanisms.

In the high-energy two-ring flips of **3** and **4**, and in the two-ring flip of **1**, the two flipping rings are mesityl or 2,6-xylyl groups. In the idealized transition states for these mechanisms, two mesityl (or 2,6-xylyl) methyl groups distal to the methine hydrogen are forced into close proximity, and this repulsive interaction is probably the most severe in the molecule.^{3b, 5a, 7} The nature of the third (nonflipping) aryl group would be expected to have relatively little effect on the energy of the transition state. Thus, the most severe steric interaction in the transition state should be very similar for **1**, **3**, and **4**, and, accordingly, so should be the free energies of activation. On the other hand, the idealized transition-state geometries for the appropriate one-ring flips differ vastly in steric encumbrance, and there is no reason to expect the barriers for stereoisomerization by this mechanism to be essentially the same for all three compounds. The observation that the activation energies in question are closely similar for **1**, **3**, and **4** therefore provides direct evidence that the high-energy exchange processes in **3** and **4** (Table II) are the result

of two-ring rather than one-ring flips. This conclusion is bolstered by empirical force field calculations,^{3b} which show that the two-ring flip is the energetically most favorable mechanism for **1**, and which yield a value of *ca.* 20 kcal/mol for the barrier to this process, in satisfactory agreement with the experimentally observed^{5a} value.

In contradistinction, in the transition states for the threshold mechanisms of **1**, **3**, and **4** (Table II), the most severe interaction is between a mesityl (or 2,6-xylyl) group and the third aryl group. The activation energy is now expected to be greatly dependent upon the nature of this third group, and this expectation is borne out, as discussed above.

A Comparison between Analogous Boranes and Methanes. The boron analogs of **2** and **3**, dimesityl-9-anthrylborane (**9**) and dimesityl-1-(2-methylnaphthyl)-borane (**10**),¹³ respectively, also stereoisomerize by the two-ring flip mechanism.⁴ The threshold barriers for the methanes are *ca.* 3–5 kcal/mol higher than those for the corresponding boranes (Table II). This difference is accounted for in part by the slightly longer C–B bond (1.58 Å in trimesitylborane⁴), as compared with the C–C bond to the central atom in triarylmethanes such as **1** (1.55 Å)^{3b} or triphenylmethane (1.53 Å).¹⁴ An increase in bond length leads to more open structures and lowered steric congestion in ground as well as transition states. Other factors assuredly play a contributory role. Thus, the three C–C–C angles about the central carbon of **4** vary from 112.1 to 117.8°,⁷ and the C–C–C angles in trimesitylmethane are computed at 117.7°,^{3b} whereas the corresponding angles in trimesitylborane are close to 120°. The somewhat smaller angles in the methanes would cause increased steric repulsion of the groups distal to the methine proton in the two-ring flip transition state. Furthermore, possible nonbonded interactions of proximal substituents with the methine proton are, of course, absent in the borane system. On the other hand, effects of (p-p) π conjugation between boron and carbon, which are absent in the methane systems, are considered negligible for triarylboraanes.⁴

Conclusion

The results of the present and related studies¹⁵ reveal that the two-ring flip is implicated in stereoisomerizations of triarylmethanes, carbenium ions, boranes, amines, and silanes. This conclusion can presumably be extended to systems in which mechanistic alternatives have not been discussed, *e.g.*, triarylgermanes,¹⁵ -phosphines,¹⁵ -arsines,¹⁵ -methyl radicals,¹⁶ *etc.* It thus appears that the two-ring flip is the stereoisomerization mechanism of lowest energy (threshold mechanism) in all systems of the type Ar_3Z and Ar_3ZX thus far examined where such isomerization occurs by correlated rotation of the aryl groups.^{5a} In addition, for systems where two-ring flip pathways for stereoisomerizations requiring higher energies are available, these pathways are evidently followed preferentially.

(13) In the comparison with **3**, it is assumed that the *p*-methyl groups of **10** have little effect on stereoisomerization barriers.

(14) P. Andersen, *Acta Chem. Scand.*, **19**, 622 (1965).

(15) For a general review, see ref 5a and 8.

(16) J. S. Hyde, R. Breslow, and C. DeBoer, *J. Amer. Chem. Soc.*, **88**, 4763 (1966); L. D. Kispert, J. S. Hyde, C. de Boer, D. LaFollette, and R. Breslow, *J. Phys. Chem.*, **72**, 4276 (1968).

Experimental Section¹⁷

Dimesityl-9-anthrylmethane (2). A solution of 9-bromoanthracene (3.0 g, 11.6 mmol) in 50 ml of anhydrous ether was treated with *n*-butyllithium (11.6 mmol, 1.9 *M* in hexane, Alfa Inorganics), at room temperature with stirring. After 10 min, chlorodimesitylmethane¹⁸ (3.3 g, 11.6 mmol) dissolved in 30 ml of dry benzene was added dropwise to the suspension of the organolithium compound, at room temperature with stirring. The mixture was refluxed for 15 min and then poured onto crushed ice. The organic layer was extracted with chloroform and dried over MgSO₄, and the solvent was distilled at reduced pressure. The crude yellow solid obtained (which was contaminated by anthracene) was recrystallized several times from ethyl acetate to yield 1.5 g (30%) of pale yellow plates, mp 248–250°. The ¹H-nmr spectrum featured resonances at $\delta_{\text{CDCl}_3}^{\text{TMS}}$ 1.28 (3 H, br s, CH₃), 1.57 (3 H, br s, CH₃), 1.73 (3 H, br s, CH₃), 2.18 (3 H, br s, CH₃), 2.23 (6 H, br s, CH₃), 6.67 (4 H, br s, aromatic H), 6.90 (1 H, s, CH), 7.30 (4 H, m, aromatic H), 7.96 (4 H, m, aromatic H), and 8.40 (1 H, s, aromatic H). Mass spectral analysis was consistent with the assigned structure; exact mass, 428.250212 (calcd, 428.250389).

Anal. Calcd for C₂₈H₃₂: C, 92.47; H, 7.53. Found: C, 92.46; H, 7.59.

Bis(2,6-xylyl)-1-(2-methylnaphthyl)methane (3). A solution of 1-bromo-2-methylnaphthalene (16.5 g, 73.5 mmol) in 100 ml of anhydrous ether was treated with *n*-butyllithium (73.5 mmol, 1.9 *M* in hexane), at room temperature with stirring. After 1 hr, bis(2,6-xylyl)chloromethane¹⁸ (19.0 g, 73.5 mmol) dissolved in 100 ml of dry benzene was added dropwise to the solution of the organolithium compound. The mixture was worked up as described above, and the crude oil obtained was distilled under vacuum to remove the volatile materials boiling below 165° at 0.1 mm. The brown residue was kugelrohr distilled (170–200°, 0.3 mm). Treatment of the resulting viscous oil with a mixture of ethanol–acetone gave a microcrystalline powder of the crude product, mp 164–170°. This product was recrystallized from a mixture of ethanol–acetone (50:50) to yield 0.82 g (3%) of white crystals, mp 172–174°. The 60-MHz ¹H-nmr spectrum displayed, in the methyl region, eight singlets which integrate for 15 protons, at $\delta_{\text{CDCl}_3}^{\text{TMS}}$ 1.52, 1.57, 1.75, 1.87, 1.92, 2.06, 2.15, and 2.23 ppm. Two singlets which integrate for a total of one proton were observed at 6.22 and 6.64 ppm, and these were assigned to the methine hydrogen of diastereomers **3b/b** and **3a/a**, respectively. A complex multiplet, which integrates for 12 protons, was observed in the aromatic region (δ 6.66–7.90 ppm). Mass spectral analysis was consistent with the assigned structure; exact mass, 364.219203 (calcd, 364.219090).

Anal. Calcd for C₂₈H₂₈: C, 92.26; H, 7.74. Found: C, 92.32; H, 7.74.

(17) Elemental analyses were performed by Schwarzkopf Micro-analytical Laboratories, Woodside, N. Y. Unless specified otherwise, nmr spectra were recorded on a Varian A-60A spectrometer at ambient temperature (ca. 37°) and refer to ca. 20% solutions in CDCl₃ containing tetramethylsilane (TMS) as internal reference. Mass spectra were obtained on an AEI MS-9 high-resolution mass spectrometer, with an ionizing voltage of 70 eV. All reactions which involved the use of organometallic compounds as reagents were carried out under a dry high-purity nitrogen atmosphere. Melting points were measured in a Thomas-Hoover apparatus and are corrected.

(18) J. Coops, W. Th. Nauta, M. J. E. Ernsting and A. C. Faber, *Recl. Trav. Chim. Pays-Bas*, **59**, 1109 (1940).

Dnmr Measurements. ¹H-nmr spectra were recorded on a Varian A-60A or Varian HA-100 spectrometer equipped with variable-temperature accessories. Temperature measurements were based on the chemical-shift separation of the protons of an ethylene glycol sample, and utilized the temperature-shift correlation of Van Geet.¹⁹ Temperatures are considered to be accurate to $\pm 2^\circ$, although within a given series of measurements smaller differences (ca. $\pm 0.5^\circ$) are considered significant. Saturation of the nmr signals was avoided. The HA-100 spectra were calibrated using the difference frequency between the lock signal and pen position (DIFF 1 of the signal monitor) as measured on the V-4315 signal counter. Unless otherwise specified, dnmr samples were ca. 25% v/v solutions with ca. 5% v/v hexamethyldisiloxane, which was used as the lock signal for the 100-MHz (frequency sweep mode) spectra. The line-shape analyses⁹ were performed on a DEC PDP-10 computer equipped with a Calcomp plotting accessory.

At 23° the 60-MHz ¹H-nmr spectrum of **2** in CHBr₃ with 1,1,1-trimethyl-3,3,3-triphenyldisiloxane as internal reference includes resonances for the four *o*-methyl groups at δ 1.16, 1.45, 1.76, and 2.06 ppm. The line-shape analysis of this spectrum and those obtained at higher temperatures was carried out as described for dimesityl-1-(2-methylnaphthyl)borane.⁴ The frequency assignments for the four diastereotopic *o*-methyl group environments are ambiguous since eight distinct assignments all give identical calculated spectra. One set of static parameters which produced a satisfactory fit to the experimental spectra was: $a = 2.06$, $b = 1.16$, $c = 1.76$, and $d = 1.45$ ppm (see Figure 3). The calculated rate constants at eight temperatures were used to calculate ΔH^\ddagger and ΔS^\ddagger from a least-squares treatment of $\ln(k/T)$ vs. $(1/T)$ ²⁰ for the enantiomerization process, and the resulting parameters were employed to derive ΔG^\ddagger for this process, as reported in the text.

The value of ΔS^\ddagger calculated for **2** was small (ca. –6 eu), but since the values obtained for ΔH^\ddagger and ΔS^\ddagger from line-shape methods are sometimes questionable,²¹ they are not reported here.

The 100-MHz ¹H-nmr spectrum of **3** in 1,2,4-trichlorobenzene with hexamethyldisiloxane as internal reference at 31° consists of ten lines in the methyl region: δ 1.41 (peak 1), 1.46 (2), 1.65 (3), 1.72 (4), 1.75 (5), 1.79 (6), 1.81 (7), 1.92 (8), 2.03 (9), and 2.08 (10) ppm. For assignments, see text.

The chemical shifts of resonances 1–10 are temperature dependent and shifts in the region of coalescence were estimated by linear extrapolation from the region where direct measurement was possible. The temperature dependence was expressed in terms of the difference in chemical shift, in Hz, of a given signal *i* and reference signal 7 as a function of temperature (*T*, °C). Good straight lines were obtained plotting $\Delta\nu_i$ against *T*. An exchange matrix for use in the Saunders computer program⁹ was constructed for a combination of the [1,2]-, [1,3]-, and [2,3]-flip mechanisms, and the ratios of rates of the four processes involved (i.e., **3b** \rightleftharpoons **3b**, **3a** \rightleftharpoons **3a**, **3b/b** \rightarrow **3a/a**, and **3a/a** \rightarrow **3b/b**) were varied as necessary to obtain a reasonable fit to the experimental spectra. For each process the rate constants derived from the line shape analysis were employed to calculate the free energies of activation at the coalescence temperature from the Eyring equation, as reported in the text.

(19) A. L. Van Geet, *Anal. Chem.*, **42**, 679 (1970); **40**, 2227 (1968).

(20) The transmission coefficient was assumed to be unity.²¹

(21) See G. Binsch, *Top. Stereochem.*, **3**, 97 (1968).